

# Spin-Free $[2]_{R12}$ Basis Set Incompleteness Correction to the Local Multireference Configuration Interaction and the Local Multireference Average Coupled Pair Functional Methods

Luke B. Roskop,<sup>†</sup> Edward F. Valeev,<sup>‡</sup> Emily A. Carter,<sup>§</sup> Mark S. Gordon,<sup>†</sup> and Theresa L. Windus<sup>\*,†</sup>

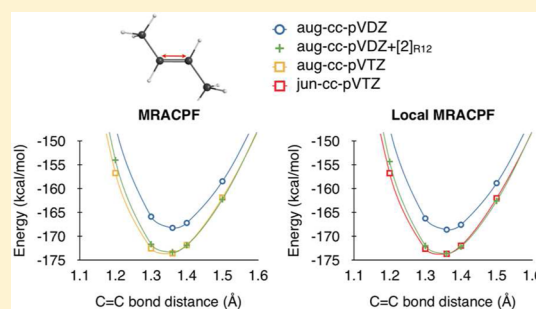
<sup>†</sup>Department of Chemistry, Iowa State University, Ames, Iowa 50010, United States

<sup>‡</sup>Department of Chemistry, Virginia Tech, Blacksburg, Virginia 24061, United States

<sup>§</sup>Department of Mechanical and Aerospace Engineering, Program in Applied and Computational Mathematics, and Andlinger Center for Energy and the Environment, Princeton University, Princeton, New Jersey 08544, United States

## Supporting Information

**ABSTRACT:** The local multireference configuration interaction (LMRCI) and local multireference averaged coupled pair functional (LMRACPF) methods are extended to include explicit correlation via the universal spin-free  $[2]_{R12}$  basis set incompleteness correction. Four test cases are examined to measure the performance of the LMRCI+ $[2]_{R12}$  (without and with the Davidson + Q correction for size-extensivity) and LMRACPF+ $[2]_{R12}$  methods. These tests examine bond dissociation energies (BDEs) for ethene, perfluoroethene, propene, and 2-butene. As has been demonstrated for other methods, the LMRCI+ $[2]_{R12}$ /LMRCI+Q+ $[2]_{R12}$ /LMRACPF+ $[2]_{R12}$  BDEs are as accurate as the conventional LMRCI/LMRACPF BDEs that are computed with the basis set one cardinal number higher. It is shown that LMRCI+ $[2]_{R12}$ /LMRCI+Q+ $[2]_{R12}$ /LMRACPF+ $[2]_{R12}$  BDEs computed with the June calendar basis sets preserve the accuracy of the corresponding BDEs computed with the conventional aug-cc-pVXZ basis sets (where X = D, T, Q).



## 1. INTRODUCTION

The high-order computational scaling that is associated with conventional *ab initio* electronic structure methods (e.g., many-body perturbation theory, configuration-interaction, and coupled-cluster) limits their application to modestly sized chemical systems. However, innovations such as the local electron correlation approximation<sup>1–5</sup> circumvent the computational overhead of the conventional methods through neglect of the interactions between electrons occupying distant pairs of localized molecular orbitals (LMOs) and neglect of excitations to localized unoccupied orbitals that are distant from a given LMO. These approximations reduce the number of wave function parameters to linear in the system size and therefore make possible the formulation of algorithms whose cost also grows linearly with the system size. Thus, local variants of wave function methods allow the treatment of larger chemical systems than is possible with the conventional counterparts. Local variants have been developed for coupled-cluster (CC) theory,<sup>6–10</sup> many-body perturbation theory,<sup>2,11–14</sup> configuration interaction (CI), and the averaged coupled pair functional (ACPF) method.<sup>15–19</sup>

Both conventional and local electron correlation methods suffer from slow decay of the basis set error, routinely expressed as  $N_{\text{bas}}^{-1}$ , where  $N_{\text{bas}}$  is the number of basis functions per atom.<sup>20,21</sup> Since the computational cost for a fixed-size system is proportional to  $N_{\text{bas}}^4$ , accurate computations on large systems

are not possible even with local methods without addressing the slow basis set convergence. The explicitly correlated R12/F12 methods<sup>22–25</sup> accelerate the basis set convergence of the correlation energy (computed with a finite basis set) to the complete basis set (CBS) limit by including terms that depend explicitly on the interelectronic distance  $r_{12}$ . These  $r_{12}$ -dependent terms approximate the short-range interelectronic behavior more effectively than the conventional two-electron excitations into the orbital basis set (OBS). The R12/F12 methodology has been shown to robustly decrease the basis set errors when combined with single-reference as well as the multireference wave functions.<sup>26</sup>

The local MP2 and local CC methods have previously been augmented with the explicitly correlated R12/F12 methods.<sup>27–34</sup> This advance is especially important to local methods since the use of large basis sets can lead to linear dependencies in the atomic orbital (AO) space<sup>35</sup> that impede orbital localization and ultimately the application of the local method. Explicit correlation with local orbital methods is an invaluable means to decrease the basis set incompleteness error (BSIE) without the numerical issues encountered with larger basis sets.

This paper presents the explicitly correlated local multireference configuration interaction (with and without the

Received: March 26, 2016

Published: June 9, 2016

Davidson + Q correction<sup>36</sup>) and local multireference averaged coupled pair functional methods (LMRCI+[2]<sub>R12</sub>, LMRCI+Q+[2]<sub>R12</sub>, and LMRACPF+[2]<sub>R12</sub>). The explicit correlation correction is determined *a posteriori* with the spin-free SF-[2]<sub>R12</sub> BSIE correction<sup>37,38</sup> (referred to herein as [2]<sub>R12</sub>) available in the massively parallel quantum chemistry program (MPQC).<sup>39</sup> Although the LMRCI and LMRACPF wave functions are different, there is no formal difference in how the [2]<sub>R12</sub> correction is computed. Note that for testing purposes local approximations were not introduced in the [2]<sub>R12</sub> correction, rather only in the MRCI/MRACPF wave function. The multiconfiguration self-consistent field (MCSCF) reference wave function and standard one-electron and two-electron integrals are generated with the GAMESS electronic structure code.<sup>40</sup> The correlated wave function (LMRCI or LMRACPF) is generated with the TigerCI code,<sup>15–18,41</sup> which is based on the symmetric group graphical approach.<sup>42–45</sup> The methodology is tested for the dissociation of ethane, perfluoroethene, propene, and 2-butene.

## 2. COMPUTATIONAL METHOD

GAMESS is used to compute the MCSCF reference wave functions and the standard one-electron and two-electron integrals that are used in the correlated wave function calculation (LMRCI or LMRACPF). The TigerCI code is used to optimize both the nonlocal and local correlated wave functions and to calculate the Davidson + Q correction. The explicitly correlated [2]<sub>R12</sub> BSIE correction is computed with MPQC using metadata that are separately generated from both GAMESS and TigerCI. The metadata (stored in disk files) contain the basis set information, coordinates, MOs, and the two-particle density matrix. New routines were added to TigerCI to generate the two-particle density matrix.

The LMOs used for the correlation calculations are as follows: inactive LMOs correspond to split-localized MOs,<sup>46</sup> active LMOs are oriented quasi-atomic orbitals,<sup>46</sup> unoccupied valence orbitals are split-localized MOs, and external orbitals are external quasi-atomic orbitals.<sup>47–49</sup> The split-localized orbitals are generated by performing an intrinsic localization procedure on the inactive nonlocal MO and unoccupied valence MO spaces separately. The active LMOs correspond to the orbitals that are required to build an MCSCF reference wave function that adequately captures the chemistry examined. For the dissociation of a bond, the active LMOs are the orbitals that describe the bonding between two atoms (e.g.,  $\sigma, \sigma^*, \pi, \pi^*$ ).

The TigerCI code uses LMO domains to determine which electronic excitations contribute to the correlation energy.<sup>16</sup> Excitations are allowed from the internal LMOs into domains of the external LMOs. Each internal LMO pair  $ij$  has a subspace domain  $[ij]$  assigned to it. To construct the orbital domains  $[ij]$ , the spatial separation between LMOs must be quantified. To this end, spheres and cylinders (with hemispherical ends) are established to define the spatial extent of the LMOs. Spheres describe the inactive and external LMOs, while cylinders correspond to active LMOs.<sup>15–17</sup> The positions of the LMO centroids (or hemispherical ends) depend on the number of atoms that strongly contribute to the LMO.<sup>16</sup> If only one atom contributes to an inactive or external LMO, then the centroid of the sphere is taken to be that atomic center. If more than one atom strongly contributes to an inactive or external LMO, then the centroid of the sphere is placed at a position determined by weighting the centers of the (strongly contributing) atoms by the degree to which they contribute to the LMO. If only one

atom strongly contributes to the LMO (inactive or external), then the radius of the atom-centered sphere is user-defined with a default value. If more than one atom contributes to an LMO, the radius of the LMO sphere is set as the distance between the two strongly contributing atoms that are the furthest apart and then scaled by a user-defined radius multiplier (scale factor).

For the two local approximations used in combination here, weak-pairs (WP)<sup>5</sup> and truncation of virtuals (TOV),<sup>1</sup> different sets of radii and radius multipliers are used to describe the LMOs. For the TOV approximation, if either of the LMOs from the strong pair  $ij$  overlaps with an external LMO (e.g., sphere–sphere, sphere–cylinder, cylinder–cylinder), then that particular external orbital is incorporated into  $[ij]$ . The WP and TOV parameters used here are listed below and are also the default parameters that are present in TigerCI.

For the WP approximation:

- 1) The WP inactive LMO sphere radius is set to 2.65 bohr, and the radius multiplier is set to 1.70.
- 2) The WP active LMO cylinder radius is set to 2.0 bohr.

For the TOV approximation:

- 1) The TOV inactive LMO sphere radius is set to 2.65 bohr, and the radius multiplier is set to 1.95.
- 2) The TOV active LMO cylinder radius is set to 2.0 bohr.
- 3) The TOV external LMO sphere radius is set to 2.65 bohr, and the radius multiplier is set to 2.0.

After the spheres and cylinders have been established, it is possible to truncate the MRCISD space as follows. In the WP approximation, for an occupied LMO pair  $ij$  to contribute to the correlation energy requires that the two LMOs (i.e., sphere–sphere, sphere–cylinder, or cylinder–cylinder) overlap. Similarly, in the TOV approximation, the unoccupied LMO (sphere) must overlap with either occupied LMO  $i$  or  $j$  (sphere–sphere, sphere–cylinder). The external LMO spheres that overlap with the internal LMO  $i$  or  $j$  spheres (or cylinders) are assigned to the  $[ij]$  domain.

The [2]<sub>R12</sub> BSIE correction is computed with MPQC and added to the conventional (local and nonlocal) MRCISD and MRACPF energies to obtain explicitly correlated results; no WP or TOV approximations were used in its evaluation. All two-electron integrals involved in the [2]<sub>R12</sub> correction were approximated using the density fitting approximation.<sup>50</sup> Evaluation of the [2]<sub>R12</sub> correction requires a two-particle density matrix, MO coefficients, and atomic coordinates. These metadata are generated from GAMESS (coordinates, MO coefficients) and TigerCI (two-particle density matrix). The two-particle density  $\Gamma_{il}^{jk}$  from the local MRACPF and the nonlocal MRACPF wave function<sup>51</sup> is computed from the following

$$\Gamma_{il}^{jk} = \frac{\langle \Psi | E_{il}^{jk} | \Psi \rangle - \langle \Psi_{\text{ref}} | E_{il}^{jk} | \Psi_{\text{ref}} \rangle}{\eta} + \langle \Psi_{\text{ref}} | E_{il}^{jk} | \Psi_{\text{ref}} \rangle$$

where  $|\Psi\rangle$  is the (L)MRACPF wave function, and  $|\Psi_{\text{ref}}\rangle$  is the reference wave function;  $E_{rs}^{pq}$  is the spin-free substitution operator defined as

$$E_{rs}^{pq} = \sum_{\sigma, \tau \in \{\alpha, \beta\}} a_{r\sigma}^{p\sigma} a_{s\tau}^{q\tau}$$

$$a_{rs}^{pq} \equiv a_p^\dagger a_q^\dagger a_s a_r$$

where  $a_q^\dagger$  and  $a_s$  are the standard creation and annihilation operators, and  $\eta$  is a scalar defined as

$$\eta = \sum_i c_i^2 g$$

where  $c_i$  is the  $i^{\text{th}}$  (L)MRACPF expansion coefficient, and  $g$  modulates the denominator (to correct size-extensivity errors)<sup>51</sup> in the ACPF energy functional

$$E_{\text{ACPF}} = \frac{\langle \Psi_{\text{ref}} + \Psi_c | H - E_0 | \Psi_{\text{ref}} + \Psi_c \rangle}{1 + g \langle \Psi_c | \Psi_c \rangle}$$

where  $|\Psi_c\rangle$  is the orthogonal (with respect to  $|\Psi_{\text{ref}}\rangle$ ) correlation function, and  $g = 2/N_{\text{elec}}$  where  $N_{\text{elec}}$  is the number of electrons.

BDEs are computed for ethene, perfluoroethene, and propene. Potential energy surfaces (PESs) for contracting and expanding the C=C bond about the MCSCF minimum are computed for 2-butene. All equilibrium and dissociated structures (supermolecules) are optimized at the MCSCF level of theory with the aug-cc-pVDZ basis set.<sup>52</sup>

LMRCISD/MRCISD with the Davidson + Q correction and LMRACPF/MRACPF energies are computed with the aug-cc-pVXZ<sup>52</sup> and jun-cc-pVXZ<sup>55</sup> basis sets (where X = D, T, Q). Compared to the aug-cc-pVXZ basis set series, the jun-cc-pVXZ basis set series removes diffuse functions from light atoms, while for heavy atoms only the highest angular-momentum diffuse function is removed. All systems are configured with the same orbitals active in both the MCSCF reference calculation and the conventional correlation calculation. As was done in previous work,<sup>54</sup> all explicitly correlated computations correlate only the strongly occupied (inactive + active) orbitals with R12 geminals.

The CBS limit of the correlation energy is estimated via the inverse power expansion<sup>20</sup> of the correlation energy based on a two-point extrapolation with correlation energies computed from the aug-cc-pVTZ and aug-cc-pVQZ basis. The aug-cc-pVQZ MCSCF energy is used to approximate the CBS reference energy.

To better compare to the literature BDE values for ethene, perfluoroethene, and propene, the 298 K binding enthalpies are computed and reported. This is accomplished by adding zero point energy and enthalpic (298 K) corrections to the  $D_e$  energies. Zero point energies and enthalpies are determined from harmonic frequencies that are computed from the MCSCF aug-cc-pVDZ Hessian. There are various sources of error that impact the computed BDEs, such as errors from the level of theory that is used to compute the correlation energy. The 298 K binding enthalpies include additional errors from the level of theory used to compute both the thermal corrections and the zero-point energies. The explicitly correlated correction (e.g.,  $[2]_{\text{R12}}$ ) is used to reduce the BSIE, however, the other errors persist in the reported BDEs.

### 3. RESULTS

**3A. Ethene.** Table 1 displays ethene [ $\text{H}_2\text{C}=\text{CH}_2(^1A_g) \rightarrow 2\text{CH}_2(^3B_1)$ ] BDEs calculated using both conventional electronic structure theory methods and explicitly correlated methods, as well as the errors in the BDEs compared to the associated CBS limits. Total energies for the equilibrium and dissociated structures (C=C bond stretched to 20 Å) can be found in Table S1 in the Supporting Information. In the correlation calculation, the 1s orbitals from the carbon atoms are frozen, the four C–H  $\sigma$  orbitals are inactive, and the C=C orbitals ( $\sigma$ ,  $\pi$ ,  $\pi^*$ ,  $\sigma^*$ ) are active orbitals. The computed BDEs at 298 K are analyzed and compared to the latest experimental/

**Table 1. Conventional and Explicitly Correlated C=C BDEs from Equilibrium and Dissociated Structures for Ethene<sup>a</sup>**

method	basis set <sup>b</sup>	conventional 298 K BDE (kcal/mol)	conventional + $[2]_{\text{R12}}$ 298 K BDE (kcal/mol)
MRACPF	aDZ	163.7 (9.9)	170.0 (3.6)
	aTZ	169.8 (3.8)	172.3 (1.3)
	aQZ	172.1 (1.5)	
	CBS <sup>c</sup>	173.6	
LMRACPF	aDZ	164.0 (9.9)	170.2 (3.7)
	aTZ	170.2 (3.7)	172.7 (1.2)
	aQZ	172.5 (1.4)	
	CBS <sup>c</sup>	173.9	
MRCI+Q	aDZ	163.9 (9.9)	170.2 (3.6)
	aTZ	170.1 (3.7)	172.7 (1.1)
	aQZ	172.7 (1.1)	
	CBS <sup>c</sup>	173.8	
LMRCI+Q	aDZ	164.2 (9.9)	170.5 (3.6)
	aTZ	170.4 (3.7)	173.0 (1.1)
	aQZ	172.7 (1.4)	
	CBS <sup>c</sup>	174.1	
MRCI	aDZ	163.1 (9.0)	169.4 (2.7)
	aTZ	168.7 (3.4)	171.3 (0.8)
	aQZ	170.8 (1.3)	
	CBS <sup>c</sup>	172.1	
LMRCI	aDZ	163.3 (9.0)	169.6 (2.7)
	aTZ	168.9 (3.4)	171.5 (0.8)
	aQZ	171.0 (1.3)	
	CBS <sup>c</sup>	172.3	

<sup>a</sup>The 298 K binding enthalpies are presented. The literature BDE is  $174.6 \pm 0.1$  kcal/mol.<sup>56</sup> The energies in parentheses are absolute errors in the BDEs relative to the associated (conventional and local) CBS values. <sup>b</sup>“aXZ” refers to the aug-cc-pVXZ basis set. <sup>c</sup> $E(\text{CBS}) = E_{\text{CASSCF}}(\text{aQZ}) + E_{\text{corr}}(\text{extrapolated})$ .

literature values ( $174.1 \pm 1.4$  kcal/mol<sup>55</sup> and  $174.60 \pm 0.10$  kcal/mol<sup>56</sup>).

Compared to the literature BDE, the LMRACPF+ $[2]_{\text{R12}}$  BDEs have errors of 4.4 and 1.9 kcal/mol for the aug-cc-pVDZ and aug-cc-pVTZ basis sets, respectively. The LMRCI+Q+ $[2]_{\text{R12}}$  BDE errors (4.1 and 1.6 kcal/mol) are slightly smaller, while the LMRCI+ $[2]_{\text{R12}}$  BDE errors are larger (5.0 and 3.1 kcal/mol) than the LMRACPF+ $[2]_{\text{R12}}$  BDE errors. Overall, the local explicitly correlated BDEs exhibit errors that are nearly the same as their corresponding nonlocal explicitly correlated BDEs.

Figure 1 displays absolute errors in the BDEs (relative to the associated CBS-extrapolated values) for the conventional and explicitly correlated methods. The explicitly correlated BDEs have similar or smaller basis set errors than the conventional BDEs that are computed with basis sets of one cardinal number higher. The deviations between the (L)MRACPF/(L)MRCI+Q aug-cc-pV(X+1)Z conventional BDEs and the aug-cc-pVXZ explicitly correlated BDEs are 0.0–0.3 kcal/mol. The (L)MRCI explicitly correlated aug-cc-pVXZ BDEs have basis set errors smaller than the conventional aug-cc-pV(X+1)Z BDEs by 0.5–0.7 kcal/mol.

Previous work on local explicitly correlated MP2 and CCSD by Werner et al.<sup>27,29</sup> noted that the inclusion of the explicit correlation greatly reduces the domain errors. Such cancellation of domain errors seems to be specific to the use of PAOs for virtual orbitals.<sup>34</sup> In the present work, standard and R12 methods have similar local truncation errors despite the use of

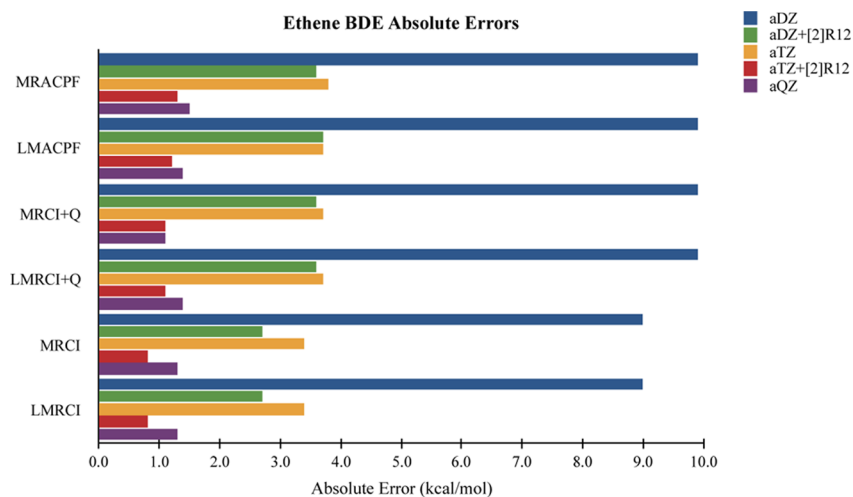


**Figure 1.** Absolute errors in the C=C BDE (kcal/mol) for ethene relative to the CBS extrapolated values. BDEs are computed with the local and nonlocal MRACPF, MRCI+Q, and MRCI methods with the aug-cc-pVDZ, the aug-cc-pVTZ, and the aug-cc-pVQZ basis sets. [2]<sub>R12</sub> results are presented for the aug-cc-pVDZ and the aug-cc-pVTZ basis sets.

PAOs. This is likely due to the use of a conventional (nonlocal) formulation of the R12 correction. Nevertheless, the local approximation errors for BDEs (0.0–0.4 kcal/mol) are significantly smaller than the residual basis set errors even after the R12 correction.

**3B. Perfluoroethene.** Table 2 displays BDEs and errors in the BDEs compared to the associated CBS limits for perfluoroethene [ $F_2C=CF_2(^1A_g) \rightarrow 2CF_2(^1A_1)$ ]. Total energies for the equilibrium and dissociated structures (C=C bond stretched to 20 Å) can be found in Table S2 in the Supporting Information. In the correlation calculation, the 1s orbitals from the carbon and fluorine atoms are frozen, there are 16 inactive orbitals, and the C=C orbitals ( $\sigma$ ,  $\pi$ ,  $\pi^*$ ,  $\sigma^*$ ) are active orbitals. There are multiple BDE values reported in the literature that are in the range 53.4–76.3 kcal/mol ( $53.4 \pm 0.7$ ,<sup>57</sup>  $69.0 \pm 2.74$ ,<sup>58</sup>  $76.3 \pm 3.0$ ,<sup>59</sup> and  $68.90 \pm 0.35$  kcal/mol<sup>56</sup>). The CBS-extrapolated MRCI, MRCI+Q, and MRACPF 298 K BDEs are 72.4, 72.9, and 68.0 kcal/mol, respectively, corresponding to the upper end of the experimental/literature range. The MRACPF value (assumed to be the best value in this work) agrees best with the literature BDEs of 69.0<sup>58</sup> and 68.90 kcal/mol.<sup>56</sup>

Figure 2 displays absolute BDE errors (relative to the associated conventional CBS extrapolated values) that are computed with the explicitly correlated and conventional methods. The (L)MRACPF and the (L)MRCI+Q explicitly correlated BDEs are more accurate than the conventional BDEs computed with basis sets that are two cardinal numbers higher. The (L)MRCI explicitly correlated BDEs exhibit smaller errors than conventional BDEs that are computed with basis sets one cardinal number higher.

**3C. Propene.** Table 3 displays BDEs and errors in the BDEs compared to the associated conventional CBS limit for propene. In the correlation calculation, the 1s orbitals from the carbon atoms are frozen, there are 7 inactive orbitals, and the C=C orbitals ( $\sigma$ ,  $\pi$ ,  $\pi^*$ ,  $\sigma^*$ ) are active. The BDEs presented here correspond to the reaction [ $CH_3CH=CH_2(^1A') \rightarrow CH_3CH:(^3A'') + :CH_2(^3A'')$ ]. Total energies for the equilibrium and dissociated structures (C=C bond stretched to 12 Å) can be found in Table S3 in the Supporting Information. A C=C bond length of 12 Å is used to model the dissociated structure since the MCSCF did not converge beyond that

**Table 2.** Conventional and Explicitly Correlated C=C BDEs from Equilibrium and Dissociated Structures for Perfluoroethene<sup>a</sup>

method	basis set <sup>b</sup>	conventional 298 K BDE (kcal/mol)		conventional + [2] <sub>R12</sub> 298 K BDE (kcal/mol)	
MRACPF	aDZ	64.3	(3.7)	67.7	(0.3)
	aTZ	65.7	(2.3)	67.3	(0.7)
	aQZ	67.0	(1.0)		
	CBS <sup>c</sup>	68.0			
LMRACPF	aDZ	64.2	(3.5)	67.5	(0.2)
	aTZ	65.7	(2.0)	67.3	(0.4)
	aQZ	66.8	(0.9)		
	CBS <sup>c</sup>	67.7			
MRCI+Q	aDZ	69.6	(3.3)	72.2	(0.7)
	aTZ	70.8	(2.1)	72.3	(0.6)
	aQZ	72.0	(0.9)		
	CBS <sup>c</sup>	72.9			
LMRCI+Q	aDZ	69.1	(3.1)	71.7	(0.5)
	aTZ	70.4	(1.8)	71.7	(0.5)
	aQZ	71.4	(0.8)		
	CBS <sup>c</sup>	72.2			
MRCI	aDZ	70.8	(1.6)	73.4	(1.0)
	aTZ	70.9	(1.5)	72.2	(0.2)
	aQZ	71.7	(0.7)		
	CBS <sup>c</sup>	72.4			
LMRCI	aDZ	70.4	(1.5)	73.0	(1.1)
	aTZ	70.5	(1.4)	71.8	(0.1)
	aQZ	71.2	(0.7)		
	CBS <sup>c</sup>	71.9			

<sup>a</sup>The 298 K binding enthalpies are presented. The experimental/literature BDEs range is 53.4–76.3 kcal/mol. The energies in parentheses are absolute errors in the BDEs relative to the associated (conventional and local) CBS values. <sup>b</sup>“aXZ” refers to the aug-cc-pVXZ basis set. <sup>c</sup> $E(\text{CBS}) = E_{\text{CASSCF}}(\text{aQZ}) + E_{\text{corr}}(\text{extrapolated})$ .

distance. The BDE value reported in the literature is  $173.46 \pm 0.29$  kcal/mol.<sup>56</sup>

Figure 3 displays absolute BDE errors (relative to the associated conventional CBS extrapolated values) that are computed with conventional and explicitly correlated methods. The (L)MRACPF and the (L)MRCI+Q explicitly correlated

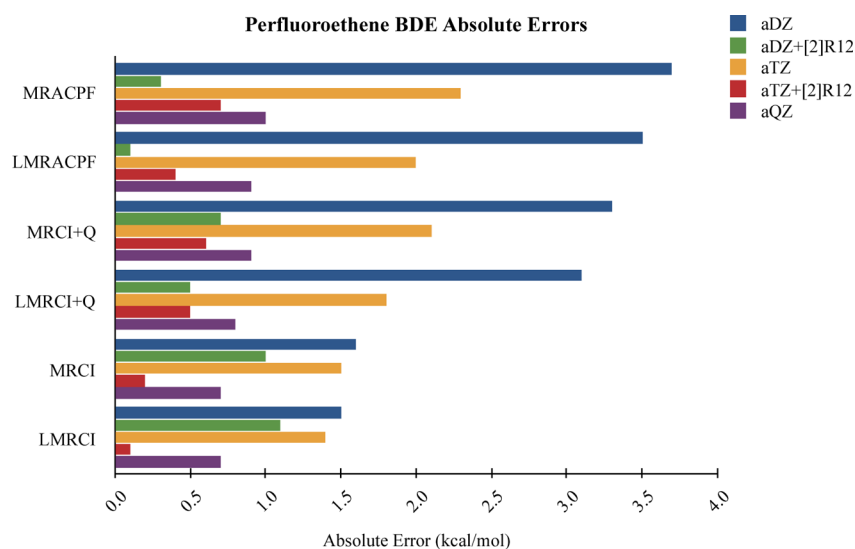


**Figure 2.** Absolute errors in the C=C BDE (kcal/mol) for perfluoroethene relative to the CBS extrapolated values. BDEs are computed with the local and nonlocal MRACPF, MRCI+Q, and MRCI methods with the aug-cc-pVDZ, aug-cc-pVTZ, and aug-cc-pVQZ basis sets.  $[2]_{R12}$  results are presented only for the aug-cc-pVDZ and aug-cc-pVTZ basis sets.

**Table 3. Conventional and Explicitly Correlated C=C BDEs from Equilibrium and Dissociated Structures for Propene<sup>a</sup>**

method	basis set <sup>b</sup>	conventional BDE (kcal/mol)		conventional + $[2]_{R12}$ BDE (kcal/mol)	
MRACPF	aDZ	163.0	(9.2)	168.8	(3.4)
	aTZ	168.9	(3.3)	171.2	(1.0)
	aQZ	170.9	(1.3)		
	CBS <sup>c</sup>	172.2			
LMRACPF	aDZ	163.5	(8.7)	169.2	(3.0)
	aTZ	169.4	(2.8)	171.7	(0.5)
	aQZ	LDAO <sup>d</sup>			
MRCI+Q	aDZ	163.6	(9.3)	169.4	(3.5)
	aTZ	169.5	(3.4)	172.0	(0.9)
	aQZ	171.6	(1.3)		
	CBS <sup>c</sup>	172.9			
LMRCI+Q	aDZ	163.9	(9.0)	169.6	(3.3)
	aTZ	169.8	(3.1)	172.2	(0.7)
	aQZ	LDAO <sup>d</sup>			
MRCI	aDZ	162.5	(8.2)	168.2	(2.5)
	aTZ	167.7	(3.0)	170.2	(0.5)
	aQZ	169.6	(1.1)		
	CBS <sup>c</sup>	170.7			
LMRCI	aDZ	162.6	(8.1)	168.4	(2.3)
	aTZ	167.8	(2.9)	170.3	(0.4)
	aQZ	LDAO <sup>d</sup>			

<sup>a</sup>The energies are computed with the (conventional) aug-cc-pVXZ basis sets. The 298 K binding enthalpies are presented. The literature BDE is  $173.5 \pm 0.3$  kcal/mol.<sup>56</sup> The energies in parentheses are absolute errors in the BDEs relative to the conventional CBS 298 K binding enthalpy value. <sup>b</sup>“aXZ” refers to the aug-cc-pVXZ basis set. <sup>c</sup> $E(\text{CBS}) = E_{\text{CASSCF}}(\text{aQZ}) + E_{\text{corr}}(\text{extrapolated})$ . <sup>d</sup>LDAO refers to linear dependency in the AO basis set.

BDEs that are computed with the aug-cc-pVDZ basis set are slightly less accurate than the conventional BDEs computed with the aug-cc-pVTZ basis set. Conversely, the MRACPF and the MRCI+Q explicitly correlated BDEs computed with the aug-cc-pVTZ basis set are more accurate than conventional BDEs computed with the aug-cc-pVQZ basis set. In addition,

the MRACPF and the MRCI+Q explicitly correlated BDEs are less accurate than their local counterpart by on average 0.4 and 0.2 kcal/mol, respectively. This discrepancy may be attributed to comparing the local BDEs to nonlocal CBS BDEs (since the local CBS BDEs are unavailable). Lastly, the MRCI and the LMRCI explicitly correlated BDEs that are computed with the aug-cc-pVDZ basis set are more accurate than the conventional BDEs that are computed with the aug-cc-pVTZ basis set.

Because of linear dependencies in the aug-cc-pVQZ basis set space, generation of a complete set (within the aug-cc-pVQZ space) of orthonormal localized orbitals is impeded, so the local aug-cc-pVQZ BDEs are unavailable. As previously shown,<sup>53</sup> the energetic inconsistencies between correlation calculations computed with the conventional Dunning basis sets (aug-cc-pVXZ) and June calendar basis sets (jun-cc-pVXZ) tend to diminish as the cardinal number (X) of the basis set increases. So, the June calendar basis sets are employed next in order to study their suitability as a substitute for the conventional Dunning basis sets when linear dependencies in the orbital basis sets are problematic.

Table 4 displays propene BDEs that are calculated with the June calendar basis sets. Total energies for the equilibrium and dissociated structures can be found in Table S4 in the Supporting Information. With respect to the LMRCI, LMRCI+Q, and LMRACPF BDEs, the differences between BDEs computed with the Dunning basis sets (Table 3) and with the June basis sets (Table 4) for X = D (T) are 1.0 (0.4), 1.0 (0.4), and 0.9 (0.9) kcal/mol, respectively, with the June basis sets having the larger error compared to their respective CBS BDEs. Further, the absolute differences between LMRACPF+ $[2]_{R12}$ , LMRCI+Q+ $[2]_{R12}$ , and LMRCI+ $[2]_{R12}$  BDEs that are computed with Dunning basis sets and June basis sets for X = D (T) are 0.1 (0.1), 0.0 (0.1), and 0.1 (0.1) kcal/mol, respectively.

As can be gleaned from Figure 4, the explicitly correlated BDEs with the June basis sets are more accurate than the conventional BDEs computed with basis sets that are one cardinal number higher. This is in contrast to aug-cc-pVXZ results in which the (L)MRACPF and the (L)MRCI+Q explicitly correlated aug-cc-pVDZ BDEs are slightly less



**Figure 3.** Absolute errors in the C=C BDE (kcal/mol) for propene relative to the CBS extrapolated values. BDEs are computed with the local and nonlocal MRACPF, MRCI+Q, and MRCI methods with the aug-cc-pVDZ, aug-cc-pVTZ, and aug-cc-pVQZ basis sets. [2]<sub>R12</sub> results are presented only for the aug-cc-pVDZ and aug-cc-pVTZ basis sets. Local aug-cc-pVQZ BDEs are unavailable due to linear dependencies in the atomic orbital basis set, which impedes the construction of a set of orthonormal localized orbitals.

**Table 4. Conventional and Explicitly Correlated C=C BDEs from Equilibrium and Dissociated Structures for Propene<sup>a</sup>**

method	basis set <sup>b</sup>	conventional BDE (kcal/mol)	conventional + [2] <sub>R12</sub> BDE (kcal/mol)
MRACPF	junDZ	162.3 (9.9)	169.0 (3.2)
	junTZ	168.5 (3.7)	171.1 (1.1)
	junQZ	170.7 (1.5)	
	CBS <sup>c</sup>	172.2	
LMRACPF	junDZ	162.6 (9.6)	169.3 (2.9)
	junTZ	168.5 (3.7)	171.6 (0.6)
	junQZ	171.3 (0.9)	
	CBS <sup>c</sup>	172.9	
MRCI+Q	junDZ	162.7 (10.2)	169.4 (3.5)
	junTZ	169.1 (3.8)	172.2 (0.7)
	junQZ	171.4 (1.5)	
	CBS <sup>c</sup>	172.9	
LMRCI+Q	junDZ	162.9 (10.0)	169.6 (3.3)
	junTZ	169.4 (3.5)	172.1 (0.8)
	junQZ	171.6 (1.3)	
	CBS <sup>c</sup>	170.7	
MRCI	junDZ	161.5 (9.2)	168.2 (2.5)
	junTZ	167.3 (3.4)	170.1 (0.6)
	junQZ	169.4 (1.3)	
	CBS <sup>c</sup>	170.7	
LMRCI	junDZ	161.6 (9.1)	168.3 (2.4)
	junTZ	167.4 (3.3)	170.2 (0.5)
	junQZ	169.5 (1.2)	

<sup>a</sup>The energies are computed with the jun-cc-pVXZ basis sets. The 298 K binding enthalpies are presented. The literature BDE is  $173.5 \pm 0.3$  kcal/mol.<sup>56</sup> The energies in parentheses are absolute errors in the BDEs relative to the conventional CBS 298 K binding enthalpy value computed with the aug-cc-pVXZ basis sets (see Table 3). <sup>b</sup>“junXZ” refers to the jun-cc-pVXZ basis set. <sup>c</sup>CBS value taken from Table 3.

accurate than the conventional aug-cc-pVTZ BDEs; however, these latter deviations are no larger than 0.2 kcal/mol.

**3D. 2-Butene.** Figure 5 displays the PESs that correspond to contracting and expanding the C=C double bond for 2-butene, with other intermolecular degrees of freedom frozen. In the correlation calculation, the 1s orbitals from the carbon

atoms are frozen, there are 10 inactive orbitals, and the C=C ( $\sigma$ ,  $\pi$ ,  $\pi^*$ ,  $\sigma^*$ ) orbitals are active. Conventional and explicitly correlated curves are computed with the aug-cc-pVDZ basis set for local and nonlocal MRCI/MRCI+Q/MRACPF. For the nonlocal MRCI, MRCI+Q, and MRACPF methods, the aug-cc-pVTZ curves were also generated. Due to complications from linear dependencies when the orthogonal LMOs are generated with the aug-cc-pVTZ basis set, the local methods (LMRCI, LMRCI+Q, and LMRACPF) employed the jun-cc-pVTZ basis set to compute the potential energy curves.

It is evident from Figure 5 that for bond lengths greater than or equal to the equilibrium C=C bond distance, the aug-cc-pVDZ+[2]<sub>R12</sub> curve overlaps closely with the aug/jun-cc-pVTZ curve for all levels of theory. For MRCI and LMRCI, the overlap between the aug-cc-pVDZ+[2]<sub>R12</sub> and triple- $\zeta$  basis set curves is slightly less than that for LMRACPF and MRACPF for bond lengths larger than equilibrium. However, the energy differences are small.

The nonparallelity errors (NPEs) for the aug-cc-pVDZ energy curves and the aug-cc-pVDZ+[2]<sub>R12</sub> energy curves relative to the nonlocal aug-cc-pVTZ energy curves and the local jun-cc-pVTZ energy curves are shown in Table 5. The NPE is defined as the difference between the maximum and minimum errors in the energy along a PES, here with respect to the triple- $\zeta$  values. Two different NPEs are reported, one that is computed from points on the PES in which the C=C bond is varied from 1.0 to 1.36 Å (equilibrium), the short-range, and another set in which the C=C bond is varied from 1.36 to 11.4 Å, the long-range.

The LMRCI, LMRCI+Q, and LMRACPF aug-cc-pVDZ NPEs for the long-range portion of the surface are significant at 4.7, 6.4, and 5.5 kcal/mol, respectively. Once explicit correlation is incorporated, the NPEs for LMRCI, LMRCI+Q, and LMRACPF aug-cc-pVDZ+[2]<sub>R12</sub> decrease to 1.1, 1.4, and 0.7 kcal/mol, respectively. A similar trend is seen for MRCI, MRCI+Q, and MRACPF.

Overall, the short-range NPEs are much larger than the long-range NPEs. The short-range NPE for the LMRCI, LMRCI+Q, and LMRACPF aug-cc-pVDZ curves are 18.2, 17.8, and 19.4

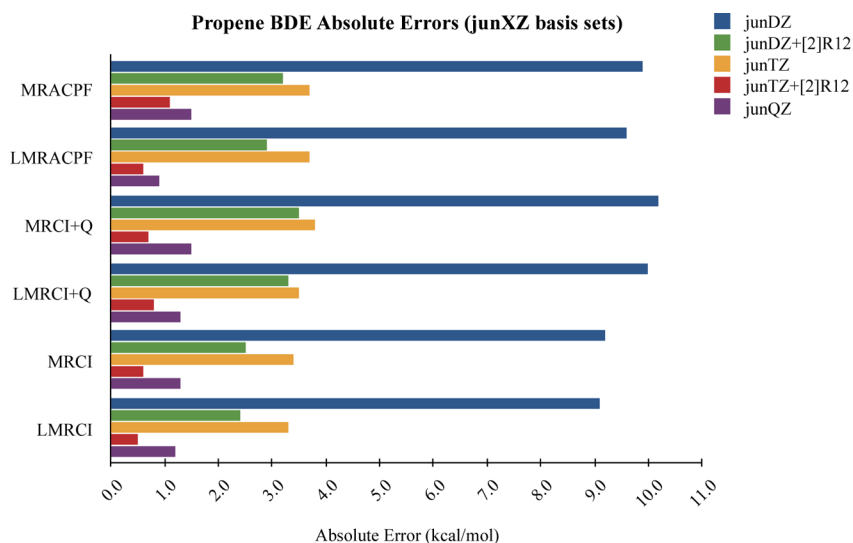


**Figure 4.** Absolute errors in the C=C BDE (kcal/mol) for propene relative to the CBS extrapolated values. BDEs are computed with the local and nonlocal MRACPF, MRCI+Q, and MRCI methods with the jun-cc-pVDZ, the jun-cc-pVTZ, and the jun-cc-pVQZ basis sets. [2]<sub>R12</sub> results are presented for the jun-cc-pVDZ and the jun-cc-pVTZ basis sets.

kcal/mol, respectively. At distances shorter than equilibrium, the atomic orbitals get distorted significantly from their “normal” shapes, and this could make both CASSCF and correlation energies harder to describe using basis sets optimized for isolated atoms and small active spaces. Comparatively, the LMRCI+[2]<sub>R12</sub>, LMRCI+Q+[2]<sub>R12</sub>, and LMRACPF+[2]<sub>R12</sub> aug-cc-pVDZ NPEs decrease substantially to 11.8, 12.1, and 13.0 kcal/mol, respectively. Conventional versus explicitly correlated LMRCI, LMRCI+Q, and LMRACPF NPEs are consistent with their nonlocal counterparts, differing by approximately 1.0 kcal/mol.

#### 4. CONCLUSIONS

The explicitly correlated LMRCI+[2]<sub>R12</sub> and LMRACPF+[2]<sub>R12</sub> methods have been assessed using the BDEs of four molecules as a metric. It was shown that explicitly correlating only the strongly occupied LMOs (inactive + active) provides reliable results, which is consistent with previous studies.<sup>54</sup> Such an approach provides a practical means to treat larger molecular systems (e.g., 2-butene).

For ethene, perfluoroethene, and propene, the LMRCI+[2]<sub>R12</sub>, LMRCI+Q+[2]<sub>R12</sub>, and LMRACPF+[2]<sub>R12</sub> BDEs computed with aug-cc-pVXZ (X = D, T) basis sets were shown to converge more rapidly to the extrapolated CBS results than the conventional approaches (LMRCI, LMRCI+Q, and LMRACPF). The LMRACPF aug-cc-pVTZ+[2]<sub>R12</sub> 298 K BDE for ethene is 172.7 kcal/mol, off by 1.9 kcal/mol compared to the literature value of 174.6 ± 0.1 kcal/mol.<sup>56</sup> For perfluoroethene, the LMRACPF aug-cc-pVTZ+[2]<sub>R12</sub> 298 K BDE is 67.3 kcal/mol, within 1.6 kcal/mol of the 68.90 ± 0.35 kcal/mol literature value.<sup>56</sup> For propene, the LMRACPF aug-cc-pVTZ+[2]<sub>R12</sub> (jun-cc-pVTZ+[2]<sub>R12</sub>) 298 K BDE is 171.7 (171.6) kcal/mol, lower by 1.8 (1.9) kcal/mol from the 173.5 ± 0.35 kcal/mol literature value.<sup>56</sup>

For propene, the aug-cc-pVXZ and jun-cc-pVXZ explicitly correlated results show good agreement (errors 0.0–0.2 kcal/mol). LMRCI, LMRCI+Q, and LMRACPF aug-cc-pVQZ BDEs are not presented since the orthogonal localization procedure employed here is unable to form a complete set of LMOs (within the aug-cc-pVQZ space) for the equilibrium

structure. This is due to linear dependencies in the AO basis set. Typically, this situation is remedied by removing the basis function that led to the numerical issue. However, this is not an attractive option since the dissociated propene structure does not exhibit the linear dependency seen in the equilibrium structure. Thus, the AO basis sets would be inconsistent between the equilibrium and dissociated structures. One solution is to also apply the orthogonal transformation that removes the linear dependency in the equilibrium structure to the dissociated structure. Another option is to employ the jun-cc-pVXZ basis sets. The latter option reduces the chances of encountering linear dependencies by reducing the diffuse functions in the basis set that typically result in these dependencies, while at the same time retaining the accuracy of the conventional aug-cc-pVQZ basis set. The LMRCI, LMRCI+Q, and LMRACPF jun-cc-pVQZ BDEs produce small energy differences compared to the MRCI, MRCI+Q, and MRACPF/aug-cc-pVQZ BDEs (errors 0.0–0.4 kcal/mol). In all fairness, it should be noted that linear dependencies could still result when using the June calendar basis set, and thus the linear dependent basis functions would need to be consistently removed across the potential energy surface.

The LMRCI+[2]<sub>R12</sub>, LMRCI+Q+[2]<sub>R12</sub>, and LMRACPF+[2]<sub>R12</sub> aug-cc-pVDZ PESs for 2-butene (Table 5) indicate faster convergence of the correlation energy than the conventional LMRCI, LMRCI+Q, and LMRACPF approaches. Compared to the local jun-cc-pVTZ PESs for 2-butene, the aug-cc-pVDZ LMRCI+[2]<sub>R12</sub>, the LMRCI+Q+[2]<sub>R12</sub>, and the LMRACPF+[2]<sub>R12</sub> (LMRCI, LMRCI+Q, and LMRACPF) NPEs for the long-range are 1.1, 1.4, and 0.7 kcal/mol (4.7, 6.4, and 5.5 kcal/mol), respectively. These NPEs indicate that the explicitly correlated aug-cc-pVDZ PESs mimic the triple- $\zeta$  basis set PESs more accurately than the conventional aug-cc-pVDZ PESs.

Overall, the convergence behaviors of explicitly correlated LMRCI+[2]<sub>R12</sub>, LMRCI+Q+[2]<sub>R12</sub>, and LMRACPF+[2]<sub>R12</sub> methods are similar. As understood from the tests presented here, it is typical for the explicitly correlated aug-cc-pVXZ+[2]<sub>R12</sub> energies (where X = D, T) to be as accurate as the

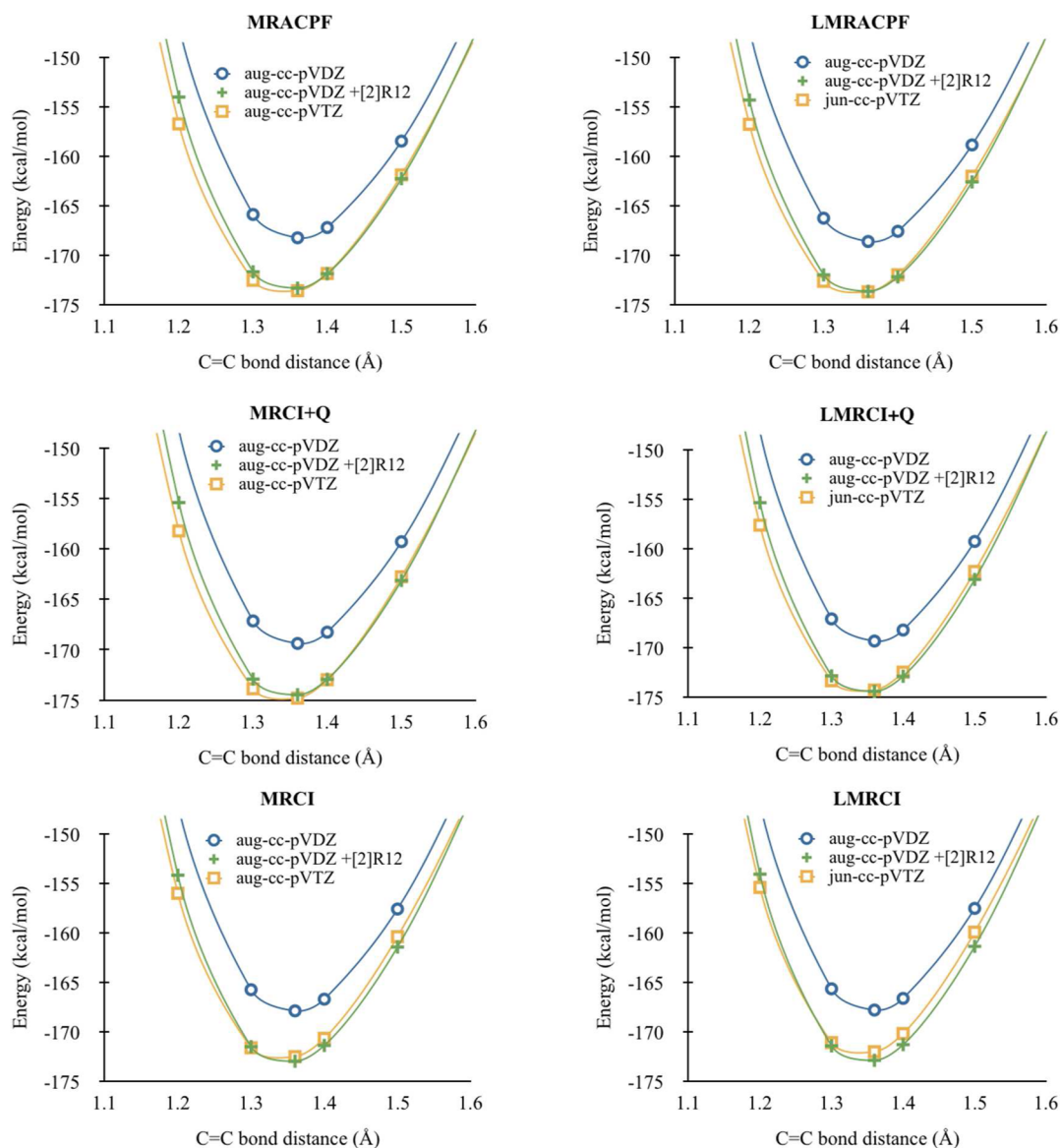


**Figure 5.** Potential energy curves (kcal/mol) in the vicinity of the MCSCF aug-cc-pVDZ C=C equilibrium bond distance for 2-butene. The aug-cc-pVDZ and aug-cc-pVDZ+[2]<sub>R12</sub> PESs are shown for MRACPF, MRCI+Q, MRCI, LMRACPF, LMRCI+Q, and LMRCI. The aug-cc-pVTZ PESs are shown for MRACPF, MRCI+Q, and MRCI. The jun-cc-pVTZ PESs are shown for LMRACPF, LMRCI+Q, and LMRCI.

**Table 5.** Nonparallelity Errors (NPEs; kcal/mol) of aug-cc-pVDZ C=C Bond Breaking PESs for 2-Butene<sup>a</sup>

method	NPE [1.0 Å–1.36 Å] (kcal/mol)		NPE [1.36 Å–11.4 Å] (kcal/mol)	
	aDZ	aDZ + [2] <sub>R12</sub>	aDZ	aDZ + [2] <sub>R12</sub>
MRACPF <sup>b</sup>	18.3	11.9	5.6	0.7
LMRACPF <sup>c</sup>	19.4	13.0	5.5	0.7
MRCI+Q <sup>b</sup>	16.9	11.2	6.4	1.4
LMRCI+Q <sup>c</sup>	17.8	12.1	6.4	1.4
MRCI <sup>b</sup>	17.5	11.2	5.0	0.9
LMRCI <sup>c</sup>	18.2	11.8	4.7	1.1

<sup>a</sup>The NPE is computed in two different regions of the PES: [1.0 Å–1.36 Å] and [1.36 Å–11.4 Å]. <sup>b</sup>NPE relative to the aug-cc-pVTZ results. <sup>c</sup>NPE relative to the jun-cc-pVTZ results.

conventional energies that are computed with the aug-cc-pV(X+1)Z basis set (one cardinal number larger).

## ■ ASSOCIATED CONTENT

### 📄 Supporting Information

The Supporting Information is available free of charge on the ACS Publications website at DOI: 10.1021/acs.jctc.6b00315.

Total energies and BDEs for the ethene, the perfluoroethene, and the propene structures (PDF)

## ■ AUTHOR INFORMATION

### Corresponding Author

\*E-mail: twindus@iastate.edu.

### Notes

The authors declare no competing financial interest.

## ■ ACKNOWLEDGMENTS

The authors thank Dr. Aaron C. West for insightful discussions and Dr. David B. Krisiloff for assistance with the TigerCI package. Funding for this research was provided by a National

Science Foundation Software Infrastructure (SI2) award, ACI-1450217 to T.L.W. and M.S.G. E.A.C. acknowledges support from National Science Foundation, award number 1265700. E.F.V. acknowledges support from the U.S. National Science Foundation awards CHE-1362655 and ACI-1047696.

## REFERENCES

- (1) Pulay, P. *Chem. Phys. Lett.* **1983**, *100*, 151.
- (2) Saebo, S.; Pulay, P. *J. Chem. Phys.* **1987**, *86*, 914.
- (3) Saebo, S.; Pulay, P. *Chem. Phys. Lett.* **1985**, *113*, 13.
- (4) Pulay, P.; Saebo, S. *Theor. Chim. Acta* **1986**, *69*, 357.
- (5) Saebo, S.; Pulay, P. *Annu. Rev. Phys. Chem.* **1993**, *44*, 213.
- (6) Hampel, C.; Werner, H.-J. *J. Chem. Phys.* **1996**, *104*, 6286.
- (7) Schütz, M.; Werner, H.-J. *Chem. Phys. Lett.* **2000**, *318*, 370.
- (8) Schütz, M. *J. Chem. Phys.* **2000**, *113*, 9986.
- (9) Schütz, M.; Werner, H.-J. *J. Chem. Phys.* **2001**, *114*, 661.
- (10) Neese, F.; Hansen, A.; Liakos, D. G. *J. Chem. Phys.* **2009**, *131*, 064103.
- (11) Schütz, M.; Hetzer, G.; Werner, H.-J. *J. Chem. Phys.* **1999**, *111*, 5691.
- (12) Hetzer, G.; Schütz, M.; Stoll, H.; Werner, H.-J. *J. Chem. Phys.* **2000**, *113*, 9443.
- (13) Maslen, P. E.; Head-Gordon, M. *Chem. Phys. Lett.* **1998**, *283*, 102.
- (14) Lee, M. S.; Maslen, P. E.; Head-Gordon, M. *J. Chem. Phys.* **2000**, *112*, 3592.
- (15) Walter, D.; Carter, E. A. *Chem. Phys. Lett.* **2001**, *346*, 177.
- (16) Walter, D.; Venkatnathan, A.; Carter, E. A. *J. Chem. Phys.* **2003**, *118*, 8127.
- (17) Venkatnathan, A.; Szilva, A. B.; Walter, D.; Gdanitz, R. J.; Carter, E. A. *J. Chem. Phys.* **2004**, *120*, 1693.
- (18) Krisiloff, D. B.; Dieterich, J. M.; Libisch, F.; Carter, E. A. Numerical Challenges in a Cholesky-Decomposed Local Correlation Quantum Chemistry Framework. In *Mathematical and Computational Modeling: With Applications in Natural and Social Sciences, Engineering, and the Arts*; Melnik, R., Ed.; John Wiley & Sons, Inc.: Hoboken, NJ, 2015. doi: 10.1002/9781118853887.ch3.
- (19) Krisiloff, D. B.; Carter, E. A. *Phys. Chem. Chem. Phys.* **2012**, *14*, 7710.
- (20) Helgaker, T.; Klopper, W.; Koch, H.; Noga, J. *J. Chem. Phys.* **1997**, *106*, 9639.
- (21) Klopper, W.; Bak, K. L.; Jørgensen, P.; Olsen, J.; Helgaker, T. *J. Phys. B: At, Mol. Opt. Phys.* **1999**, *32*, R103.
- (22) Shiozaki, T.; Knizia, G.; Werner, H.-J. *J. Chem. Phys.* **2011**, *134*, 034113.
- (23) Haunschild, R.; Cheng, L.; Mukherjee, D.; Klopper, W. *J. Chem. Phys.* **2013**, *138*, 211101.
- (24) Demel, O.; Kedzuch, S.; Svana, M.; Ten-no, S.; Pittner, J.; Noga, J. *Phys. Chem. Chem. Phys.* **2012**, *14*, 4753.
- (25) Ten-no, S.; Noga, J. *WIREs Comput. Mol. Sci.* **2012**, *2*, 114.
- (26) Liu, W.; Hanauer, M.; Köhn, A. *Chem. Phys. Lett.* **2013**, *565*, 122.
- (27) Werner, H.-J. *J. Chem. Phys.* **2008**, *129*, 101103.
- (28) Adler, T. B.; Werner, H.-J.; Manby, F. R. *J. Chem. Phys.* **2009**, *130*, 054106.
- (29) Adler, T. B.; Werner, H.-J. *J. Chem. Phys.* **2009**, *130*, 241101.
- (30) Tew, D. P.; Helmich, B.; Hättig, C. *J. Chem. Phys.* **2011**, *135*, 074107.
- (31) Pavosevic, F.; Neese, F.; Valeev, E. F. *J. Chem. Phys.* **2014**, *141*, 054106.
- (32) Schmitz, G.; Hattig, C.; Tew, D. *Phys. Chem. Chem. Phys.* **2014**, *16*, 22167.
- (33) Ma, Q.; Werner, H.-J. *J. Chem. Theory Comput.* **2015**, *11*, S291.
- (34) Pavosevic, F.; Pinski, P.; Riplinger, C.; Neese, F.; Valeev, E. F. *J. Chem. Phys.* **2016**, *144*, 144109.
- (35) Subotnik, J. E.; Dutoi, A. D.; Head-Gordon, H. *J. Chem. Phys.* **2005**, *123*, 114108.
- (36) Langhoff, S. R.; Davidson, E. R. *Int. J. Quantum Chem.* **1974**, *8*, 61.
- (37) Torheyden, M.; Valeev, E. F. *J. Chem. Phys.* **2009**, *131*, 171103.
- (38) Kong, L.; Valeev, E. F. *J. Chem. Phys.* **2011**, *135*, 214105.
- (39) Janssen, C. L.; Nielsen, I. B.; Leininger, M. L.; Valeev, E. F.; Seidl, E. T. *The Massively Parallel Quantum Chemistry Program (MPQC)*, Version 3.0 (alpha); Sandia National Laboratories: Livermore, CA, 2009.
- (40) Schmidt, M. W.; Baldridge, K. K.; Boatz, J. A.; Elbert, S. T.; Gordon, M. S.; Jensen, J. J.; Koseki, S.; Matsunaga, N.; Nguyen, K. A.; Su, S.; Windus, T. L.; Dupuis, M.; Montgomery, J. A. *J. Comput. Chem.* **1993**, *14*, 1347–1363. Gordon, M. S.; Schmidt, M. W. Advances in Electronic Structure Theory: GAMESS a Decade Later. In *Theory and Applications of Computational Chemistry*; Dykstra, C. E., Frenking, G., Kim, K. S., Scuseria, G. E., Eds.; Elsevier: Amsterdam, The Netherlands, 2005; Chapter 41.
- (41) <https://github.com/EACcodes/TigerCI> (accessed June 1, 2016).
- (42) Duch, W.; Karwowski, J. *Int. J. Quantum Chem.* **1982**, *22*, 783.
- (43) Duch, W.; Karwowski, J. *Comput. Phys. Rep.* **1985**, *2*, 93.
- (44) Duch, W. *Int. J. Quantum Chem.* **1985**, *27*, 59.
- (45) Duch, W. *GRMS or Graphical Representation of Model Spaces*; Springer: Berlin, 1986.
- (46) West, A. C.; Schmidt, M. W.; Gordon, M. S.; Ruedenberg, K. J. *Phys. Chem. A* **2015**, *119*, 10360.
- (47) Bytautas, L.; Ivanić, J.; Ruedenberg, K. *J. Chem. Phys.* **2003**, *119*, 8217.
- (48) West, A. C.; Schmidt, M. W.; Gordon, M. S.; Ruedenberg, K. J. *Chem. Phys.* **2013**, *139*, 234107.
- (49) West, A. C. *Comput. Theor. Chem.* **2014**, *1045*, 73.
- (50) Manby, F. J. *J. Chem. Phys.* **2003**, *119*, 4607.
- (51) Gdanitz, R. J.; Ahlrichs, R. *Chem. Phys. Lett.* **1988**, *143*, 413 (1988)..
- (52) Dunning, T. H., Jr. *J. Chem. Phys.* **1989**, *90*, 1007. Kendall, R. A.; Dunning, T. H., Jr.; Harrison, R. J. *J. Chem. Phys.* **1992**, *96*, 6796.
- (53) Papajak, E.; Leverentz, H. R.; Zheng, J.; Truhlar, D. G. *J. Chem. Theory Comput.* **2009**, *5*, 1197. Papajak, E.; Truhlar, D. G. *J. Chem. Theory Comput.* **2010**, *6*, 597. Papajak, E.; Zheng, J.; Xu, X.; Leverentz, H. R.; Truhlar, D. G. *J. Chem. Theory Comput.* **2011**, *7*, 3027. Zheng, J.; Xu, X.; Truhlar, D. G. *Theor. Chem. Acc.* **2011**, *128*, 295. Papajak, E.; Truhlar, D. G. *J. Chem. Theory Comput.* **2011**, *7*, 10.
- (54) Roskop, L. B.; Kong, L.; Valeev, E. F.; Gordon, M. S.; Windus, T. L. *J. Chem. Theory Comput.* **2014**, *10*, 90.
- (55) Lide, D. R. *Handbook of Chemistry and Physics*; CRC: Boca Raton, FL, 2001.
- (56) Ruscic, B.; Pinzon, R. E.; Morton, M. L.; von Laszewski, G.; Bittner, S.; Nijsure, S. G.; Amin, K. A.; Minkoff, M.; Wagner, A. F. *J. Phys. Chem. A* **2004**, *108*, 9979. Ruscic, B.; Pinzon, R. E.; von Laszewski, G.; Kodeboyina, D.; Burcat, A.; Leahy, D.; Montoya, D.; Wagner, A. F. *J. Phys.: Conf. Ser.* **2005**, *16*, 561.
- (57) Lias, S. G.; Liebman, J. F.; Levin, R. D. *J. Phys. Chem. Ref. Data* **1984**, *13*, 695.
- (58) Berman, D.; Bomse, D. S.; Beauchamp, J. L. *Int. J. Mass Spectrom. Ion Phys.* **1981**, *39*, 263.
- (59) Zmbov, K. F.; Uy, O. M.; Margrave, J. L. *J. Am. Chem. Soc.* **1968**, *90*, 5090.